



Noninvasive assessment of paediatric hepatic steatosis by using attenuation imaging

Sook Min Hwang¹ · Ky Young Cho²

Received: 12 November 2022 / Revised: 20 April 2023 / Accepted: 26 April 2023 / Published online: 17 May 2023
© The Author(s), under exclusive licence to European Society of Radiology 2023

Abstract

Objectives To evaluate the diagnostic performance of attenuation imaging (ATI) with an ultrasound scanner (US) in the detection of paediatric hepatic steatosis.

Methods Ninety-four prospectively enrolled children were classified into normal weight and overweight/obese (OW/OB) groups according to body mass index (BMI). US findings, including hepatic steatosis grade and ATI value, were examined by two radiologists. Anthropometric and biochemical parameters were obtained, and nonalcoholic fatty liver disease (NAFLD) scores, including the Framingham steatosis index (FSI) and hepatic steatosis index (HSI), were calculated.

Results After screening, 49 OW/OB and 40 normal weight children aged 10–18 years old (55 males and 34 females) participated in this study. The ATI value was significantly higher in the OW/OB group than in the normal weight group and showed a significant positive correlation with BMI, serum alanine transferase (ALT), uric acid, and NAFLD scores ($p < 0.05$). In the multiple linear regression adjusted for age, sex, BMI, ALT, uric acid, and HSI, ATI showed a significant positive association with BMI and ALT ($p < 0.05$). The receiver operating characteristic analysis showed a very good ability of ATI to predict hepatic steatosis. The intraclass correlation coefficient (ICC) of interobserver variability was 0.92, and the ICCs of intraobserver variability were 0.96 and 0.93 ($p < 0.05$). According to the two-level Bayesian latent class model analysis, the diagnostic performance of ATI showed the best performance for predicting hepatic steatosis among other known non-invasive NAFLD predictors.

Conclusions This study suggests that ATI is an objective and possible surrogate screening test for detecting hepatic steatosis in paediatric patients with obesity.

Clinical relevance statement Using ATI as a quantitative tool in hepatic steatosis allows clinicians to estimate the extent of the condition and track changes over time. This is helpful for monitoring disease progression and guiding treatment decisions, especially in paediatric practice.

Key Points

- Attenuation imaging is a noninvasive US-based method for the quantification of hepatic steatosis.
- Attenuation imaging values were significantly higher in the OW/OB and steatosis groups than in the normal weight and no steatosis groups, respectively, with a meaningful correlation with known clinical indicators of nonalcoholic fatty liver disease.
- Attenuation imaging performs better than other noninvasive predictive models used to diagnose hepatic steatosis.

Keywords Child · Obesity · Nonalcoholic fatty liver disease · Observer variation

Abbreviations

AC	Attenuation coefficient
ALP	Alkaline phosphatase
ALT	Alanine transferase
AST	Aspartate aminotransferase
ATI	Attenuation imaging
AUC	Area under the ROC curve
BMI	Body mass index
CAP	Controlled attenuation parameter
FSI	Framingham steatosis index

✉ Ky Young Cho
choky96@hallym.or.kr

¹ Department of Radiology, Hallym University Kangnam Sacred Heart Hospital, Seoul 07441, Korea

² Department of Pediatrics, Hallym University Kangnam Sacred Heart Hospital, 1 Singil-ro, Yeongdeungpo-gu, Seoul 07441, Korea

GGT	Gamma-glutamyl transpeptidase
HDL	High-density lipoprotein
HSI	Hepatic steatosis index
Ht	Height
ICC	Intraclass correlation coefficient
LCA	Latent class model analysis
LDL	Low-density lipoprotein
MRI-PDFP	MRI-proton density fat fraction
MRS	MR spectroscopy
NAFLD	Nonalcoholic fatty liver disease
NASH	Nonalcoholic steatohepatitis
OW/OB	Overweight/obese
ROC	Receiver operating characteristic
TG	Triglyceride
WC	Waist circumference

Introduction

Paediatric obesity is a major personal and societal health problem [1], and the prevalence of nonalcoholic fatty liver disease (NAFLD) is approximately 26–59% among obese children [2, 3]. The well-known cause of NAFLD is obesity, and especially during the COVID-19 pandemic period, school closures and increased desk-bound behaviour have been major factors related to the increase in NAFLD [4, 5]. According to Feldstein AE et al, children with NAFLD have a significantly shorter life expectancy and approximately 13.8-fold higher mortality related to end-stage liver disease than the general population of the same sex and age [6]. They also found that some patients progressed to liver fibrosis, but this fibrosis was not detected on the initial liver biopsy specimen a short period before. A small percentage of these patients may have advanced fibrosis requiring tertiary care and may develop hepatocellular carcinoma [2, 7]. NAFLD is a progressive disease, and early detection of NAFLD is important, especially in children with a long remaining life expectancy.

To date, liver biopsy has been considered the gold standard for diagnosing NAFLD [8]. However, liver biopsy is not easy to perform on paediatric patients because of the associated invasiveness and the risk of bleeding and the intra- and interobserver variability in specimen readings. Additionally, it is not practical for screening and follow-up purposes [1, 8]. Regarding imaging, ultrasound (US) is the most widely used modality for screening and assessing hepatic steatosis [1, 8]. However, US also has a few weaknesses, including subjective characteristics of examination, qualitative evaluation, intra- and interobserver variability, poor ability to detect mild steatosis, and its nonquantitative imaging methodology [9, 10]. As a consequence, an objective and quantitative surrogate evaluation method is needed for the detection and follow-up care of NAFLD in children.

Attenuation imaging (ATI) measures the characteristics of US beam attenuation in specific tissues. Regarding hepatic steatosis, as the degree of fatty infiltration increases, the attenuation also increases [11]. ATI produces an attenuation coefficient (AC), which corresponds to the change in US beam intensity with the depth of US images [8]. With these characteristics, ATI is a promising noninvasive method for measuring the degree of fat accumulation in the liver. However, few studies have investigated the utility of ATI for the evaluation of fatty liver in paediatric patients.

Therefore, the purpose of this study was to evaluate the diagnostic performance and inter- and intraobserver variability of ATI in the detection of hepatic steatosis compared with the various other noninvasive predictive models used to diagnose hepatic steatosis.

Methods

Study design and patients

In this cross-sectional study, we recruited 94 children to evaluate the diagnostic performance of ATI with US from September 2019 to March 2022 at a single centre. The subjects were divided into two groups according to BMI: the normal weight and overweight/obese (OW/OB) groups. The OW/OB group included patients with BMIs that exceeded the 85th percentile for their age and sex, and the normal weight group included patients with BMIs < 75th percentile based on the 2017 Korean growth chart [12]. Furthermore, based on the presence or absence of hepatic steatosis in US, we divided the patients into two groups: the no steatosis and steatosis groups. The study protocol was approved by the ethics committee of the Hallym University Kangnam Sacred Heart Hospital (reference number 2022-05-005). Information regarding the US and the risks and benefits related to US was given to the parents of each child. Written informed consent was obtained from all the participants and their parents on behalf of any participants under the age of 18 years old prior to the start of the study.

Inclusion and exclusion criteria

The inclusion criteria of the OW/OB group were as follows: (a) patients under 18 years of age and (b) children referred to our institution for obesity by a paediatric clinician who specialised in childhood obesity and scheduled for abdominal US examination. The exclusion criteria were as follows: (a) individuals with a history of liver disease, (b) individuals with focal lesions in the liver, and (c) patients with difficulty measuring ATI in US due to difficulty of breath holding.

The inclusion criteria of the normal weight group were as follows: (a) patients under 18 years of age and

(b) children referred to US examination from the outpatient clinic of the paediatric department of our institution for abdominal pain. The exclusion criteria were as follows: (a) individuals with history of liver disease, (b) individuals with focal lesions in liver, and (c) patients with difficulty measuring ATI in US due to difficulty of breath holding.

Anthropometric and blood biochemical parameters and NAFLD scores

The anthropometric parameters of the participants included height (Ht), weight, BMI, waist circumference (WC), and blood pressure. Blood biochemical parameters included fasting blood glucose, 25(OH)-vitamin D, uric acid, liver function tests, including aspartate aminotransferase (AST), ALT, and gamma-glutamyl transpeptidase (GGT), and lipid profiles, including total cholesterol, high-density lipoprotein (HDL) cholesterol, low-density lipoprotein (LDL) cholesterol, and triglycerides (TGs). The Framingham steatosis index (FSI) and hepatic steatosis index (HSI) NAFLD scores were obtained using established formulas [13, 14].

Hepatic steatosis grade and ATI examination

All ATI examinations were performed with an US scanner equipped with a 1–8-MHz convex probe on an Aplio i900 system (Canon Healthcare) by two radiologists with 12 and 3 years of experience in paediatric US imaging at the same time. The patients fasted for at least 6 h prior to undergoing ATI, and both operators were blinded to the clinical details of the patients, except for their apparent body shape. In this study, mild steatosis was defined as the presence of hyperechogenicity of the liver parenchyma and increased hepatorenal contrast with US features. Moderate steatosis was defined as both hyperechogenicity of the liver parenchyma and increased hepatorenal contrast, as well as blurred vessel wall echogenicity. Severe steatosis was defined when, in addition to the criteria for moderate steatosis, there was posterior beam attenuation obscuring the diaphragm margin (Fig. 1) [9, 15, 16]. ATI examinations were performed on the right lobe through an intercostal window with the transducer perpendicular to the skin. After setting an adequate sonic window on the grey-scale ultrasound image, an ATI examination was performed. A fan-shaped sampling box measuring 2×4 cm or larger was positioned in the hepatic parenchyma while the breath was held. The sampling box was located at least 2 cm below the

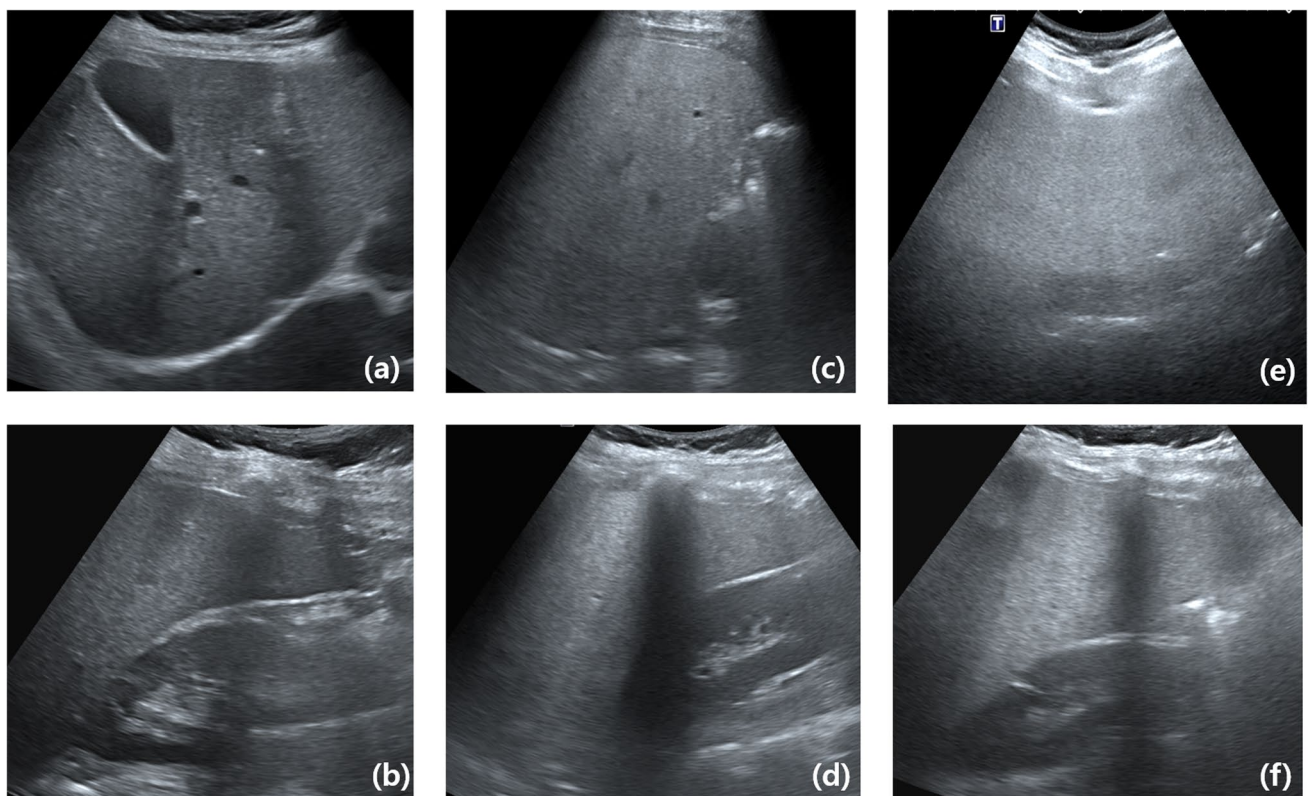


Fig. 1 US images of mild (a, b), moderate (c, d), and severe (e, f) hepatic steatosis

liver capsule to avoid reverberation artefacts (Fig. 2). On the ATI examination, a conventional greyscale ultrasound image is shown on the left side, and the same ultrasound image overlain with an attenuation map is simultaneously shown on the right side. The degree of attenuation was colour-coded and demonstrated in the sampling box. Structures such as blood vessels or areas with reverberation artefacts cause significant errors in the attenuation calculation and are excluded from the attenuation map. In the lower-left corner, the attenuation coefficient and the goodness of fit (R^2) are presented. The AC value, which is dB/cm/MHz, is displayed. Additionally, the reliability of the result was displayed as an R^2 value. The R^2 values were categorised into poor ($R^2 < 0.80$), good ($0.80 \leq R^2 < 0.90$), or excellent ($R^2 > 0.90$). ACs with $R^2 \geq 0.80$ were regarded as valid measurements. ATI examinations were performed until five valid measurements were obtained, and the median value among the obtained results was used. In each patient, all measurements were performed at the same intercostal sonic window while the patient held his or her breath.

Statistical analysis

The Shapiro–Wilk test was used to assess the normal distribution of continuous variables. The normally distributed data were analysed using the t test and are presented as the means and standard deviations. The nonnormally distributed data were analysed using Wilcoxon’s rank sum test and are presented as medians and interquartile ranges. Categorical variables were analysed by the chi-square test and are presented as frequencies and percentages. For a two-sample t test with a power of 0.8, a significance level of 0.05, and an effect size of 0.55 from the previous study, a sample size of 45 per group was determined using G*Power (version 3.1.9.7) [17]. Pearson’s correlation coefficient was used to

test the association between two quantitative continuous variables. A correlogram was constructed using the corrplot package. The linear regression and receiver operating characteristic (ROC) analysis used variables showing a significant difference between the normal and OW/OB groups in the univariate analysis. Stepwise multiple linear regression used backward elimination methods. The diagnostic performance of ATI in predicting hepatic steatosis detected by US was analysed by the ROC analysis, and the results were compared with other NAFLD scores using the pROC package. Inter- and intraobserver variability was analysed by the ICC package. In the absence of the gold standard test, such as liver biopsy, we used a two-level Bayesian latent class model analysis (LCA) with discrete latent variables to evaluate the diagnostic performance and accuracy of ATI for predicting hepatic steatosis. The data were analysed by R (version 4.1.2), Prism (version 9.4.1), and the MICE website [18]. Statistical significance was declared at a p value < 0.05 .

Results

Patient characteristics

This prospective study was conducted among participants who met the inclusion criteria. Five patients in the normal weight group were excluded for the following reasons: abnormal findings on US (2 haemangiomas, 1 focal nodular hyperplasia, calcified nodular lesion, and 1 poor cooperation). After screening, 49 OW/OB (38 males and 11 females, mean age 12.24 years) and 40 normal weight (17 males and 23 females, mean age 15.25 years) children participated in this study. There were 41 children in the no steatosis group on US (16 males and 25 females, mean age 15.17 years)

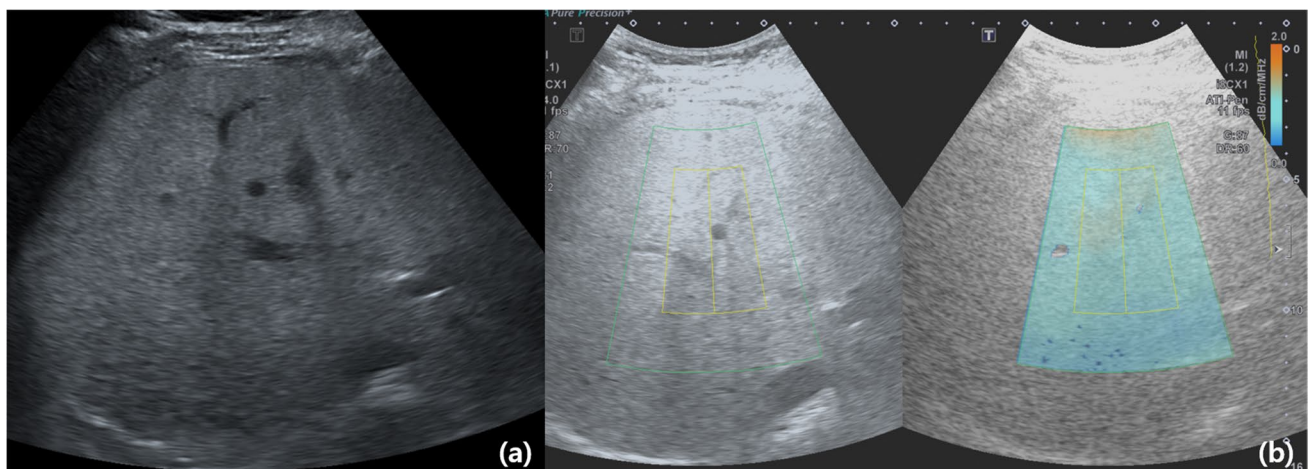


Fig. 2 Performance of ultrasound attenuation imaging. After setting an adequate greyscale ultrasound image (a), an ATI examination was performed (b)

and 48 children in the steatosis group on US (39 males and 9 females, mean age 12.29 years). The characteristics of the participants are presented in Table 1. As expected, the weight, BMI, WC, and WC-to-Ht ratio in the OW/OB group were significantly higher than those in the normal weight group ($p < 0.05$, Table 1). For the blood biochemical profile,

the OW/OB group showed significantly higher levels of glucose, uric acid, AST, ALT, AST-to-ALT ratio, GGT, total cholesterol, TGs, LDL cholesterol, and 25-OH vitamin D than the normal weight group ($p < 0.05$, Table 1).

Regarding the prevalence of hepatic steatosis detected by US, a significantly higher grade was detected in the OW/OB

Table 1 Characteristics of participants in the normal weight and overweight/obesity groups

	Normal weight ($N=40$)	Overweight/obesity ($N=9/40$)	p value
Demographic findings			
Age (years)	15.25 [12.09; 16.74]	12.24 [10.97; 14.88]	0.009
Male	17 (42.50%)	38 (77.55%)	0.002
Anthropometric measurements			
Weight (kg)	49.00 [43.10; 57.20]	66.30 [58.70; 76.10]	<0.001
Weight (z score)	-0.40 ± 1.29	2.01 ± 1.00	<0.001
Height (cm)	160.32 ± 10.97	158.97 ± 11.22	0.570
Height (z score)	0.25 ± 1.19	0.60 ± 1.27	0.184
BMI (kg/m^2)	19.31 ± 3.02	27.12 ± 3.02	<0.001
BMI (z score)	$-0.42 [-1.98; 0.31]$	$2.04 [1.67; 2.48]$	<0.001
WC (cm)	68.00 [63.00; 72.20]	89.00 [84.50; 97.75]	<0.001
WC-to-height ratio	0.43 ± 0.06	0.57 ± 0.004	<0.001
Systolic BP (mmHg)	110.0 [104.0; 119.0]	110.0 [108.0; 120.0]	0.151
Diastolic BP (mmHg)	65.5 [60.5; 70.0]	62.0 [61.0; 70.0]	0.579
Blood biochemical profiles			
Glucose (mg/dL)	96.50 [90.00; 100.50]	98.00 [91.00; 102.00]	0.517
Uric acid (mg/dL)	5.23 ± 1.53	6.53 ± 1.76	<0.001
AST (IU/L)	21.50 [19.00; 31.00]	40.00 [28.00; 54.00]	<0.001
ALT (IU/L)	13.00 [9.00; 27.50]	64.00 [35.00; 107.00]	<0.001
AST-to-ALT ratio	1.74 [1.21; 2.22]	0.63 [0.54; 0.79]	<0.001
γ -GT (IU/L)	12.00 [11.00; 19.50]	27.00 [21.00; 41.00]	<0.001
Total cholesterol (mg/dL)	155.00 ± 34.64	171.84 ± 30.94	0.019
Triglycerides (mg/dL)	79.00 [64.50; 110.00]	110.50 [90.50; 157.00]	0.001
HDL cholesterol (mg/dL)	48.85 ± 10.56	45.50 ± 9.50	0.169
LDL cholesterol (mg/dL)	89.50 ± 24.31	110.00 ± 26.80	0.002
25-OH vitamin D (ng/mL)	25.47 ± 5.84	17.47 ± 6.06	0.037
Radiologic findings by US			
Liver steatosis grade			<0.001
No	36 (90.00%)	5 (10.20%)	
Mild	4 (10.00%)	5 (10.20%)	
Moderate	0 (0.00%)	34 (69.39%)	
Severe	0 (0.00%)	5 (10.20%)	
Attenuation imaging value			
Observer 1	0.50 ± 0.11	0.72 ± 0.13	<0.001
Observer 2	0.47 ± 0.09	0.71 ± 0.13	<0.001
NAFLD score			
Hepatic steatosis index	26.36 [22.70; 29.08]	39.69 [36.90; 42.85]	<0.001
Framingham steatosis index	3.04 [1.98; 4.46]	41.26 [28.79; 56.13]	<0.001

Data are expressed as the means \pm standard deviations or medians (interquartile ranges) or n (%). p values were obtained from the Student t test, Wilcoxon rank-sum test, or chi-square test comparing the normal weight and overweight/obesity groups. *BMI*; body mass index; *WC*, waist circumference; *BP*, blood pressure; *AST*, aspartate aminotransferase; *ALT*, alanine aminotransferase; *γ -GT*, gamma-glutamyl transferase; *HDL*, high-density lipoprotein; *LDL*, low-density lipoprotein; *US*, ultrasound; *NAFLD*, nonalcoholic fatty liver disease

group than in the normal weight group ($p < 0.05$, Table 1 and Fig. 3A). In the OW/OB group, hepatic steatosis above grade 1 was detected in 44 participants (91.67%). The ATI values of observers 1 and 2 in the OW/OB group were significantly higher than those in the normal group ($p < 0.05$, Table 1 and Fig. 3B). The NAFLD scores, including the HSI and FSI, were significantly higher in the OW/OB group than in the normal weight group ($p < 0.05$, Table 1).

The characteristics of participants with and without steatosis detected with US

In this study, the no steatosis group was defined as no detectible hepatic steatosis with US, and the steatosis group was defined as children with hepatic steatosis of more than a mild degree according to US. A total of 41 children were included in the no steatosis group, and 48 children were included in the steatosis group. The prevalence of steatosis was significantly higher in the OW/OB group (91.7%) than in the normal group (12.2%) ($p < 0.001$, Table 2). The weight, BMI, WC, and WC-to-Ht ratio in the steatosis group were significantly higher than those in the no steatosis group ($p < 0.05$, Table 2). Regarding the blood biochemical profile, the steatosis group showed significantly higher levels of uric acid, AST, ALT, AST-to-ALT ratio, GGT, total cholesterol, TGs, LDL cholesterol, and 25-OH vitamin D than the normal weight group ($p < 0.05$, Table 2).

In the steatosis group, 9 (18.75%), 34 (70.83%), and 5 (10.42%) children showed mild, moderate, and severe degrees, respectively. The ATI values of observers 1 and 2 in the steatosis group were significantly higher than those in the no steatosis group ($p < 0.05$, Table 2 and Fig. 3C). The NAFLD scores, including the HSI and FSI, were significantly higher in the steatosis group than in the no steatosis group ($p < 0.05$, Table 2).

The correlations among the anthropometric and blood biochemical parameters, US findings, and NAFLD scores in the normal and OW/OB groups

The correlogram in Fig. 4 displays positive correlations in blue and negative correlations in red for significant correlations between variables ($p < 0.05$). The intensity of the colour is proportional to the correlation coefficients.

Regarding the US findings, the hepatic steatosis grade and ATI showed a significant positive correlation with BMI, WC, WC-to-Ht ratio, ALT, TGs, uric acid, and NAFLD scores, including the HSI and FSI ($p < 0.05$, Fig. 4). Regarding relationships with the hepatic steatosis grade detected by US, the highest significant positive coefficient was observed for FSI (0.74), and the highest significant negative coefficient was observed for the AST-to-ALT ratio (-0.66) ($p < 0.05$, Fig. 4). Regarding the relationships with ATI in US, the WC-to-Ht ratio showed the highest significant positive coefficient (0.42), and the AST-to-ALT ratio had the highest significant negative coefficient (-0.30) ($p < 0.05$, Fig. 4).

Regarding the anthropometric measures, BMI and WC showed a significant negative correlation with the AST-to-ALT ratio and vitamin D values and a significant positive correlation with the US findings, including the hepatic steatosis grade and ATI, and the NAFLD scores, including the HSI and FSI ($p < 0.05$, Fig. 4). Regarding the blood biochemical profiles, the AST-to-ALT ratio showed a negative correlation with BMI, WC, US findings, including the hepatic steatosis grade and ATI, NAFLD scores, uric acid, and TGs ($p < 0.05$, Fig. 4). Significant positive correlations were found between ALT and BMI, WC, US findings, including the hepatic steatosis grade and ATI, and NAFLD scores, including HSI and FSI ($p < 0.05$, Fig. 4).

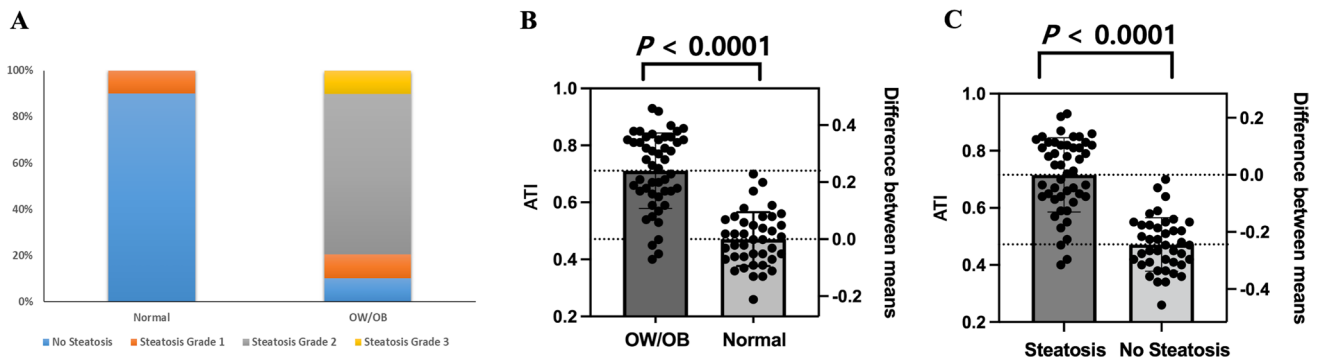


Fig. 3 A The prevalence of hepatic steatosis detected in abdominal ultrasonography according to the steatosis grade in the normal and overweight/obesity (OW/OB) groups. The distribution of attenuation

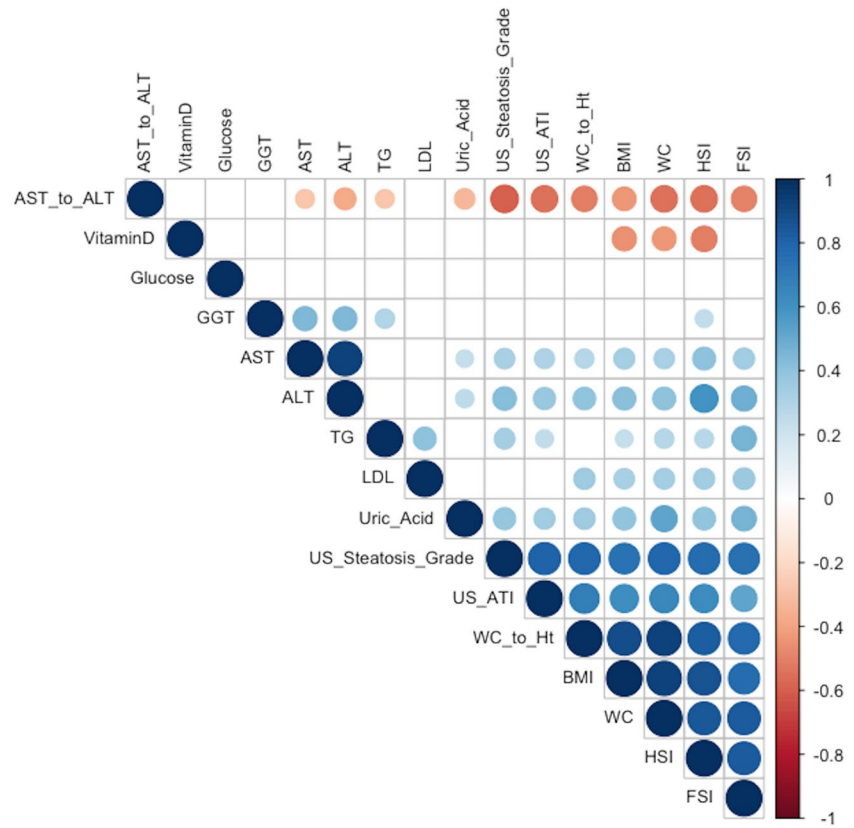
imaging values (ATI) between the normal and overweight/obesity (OW/OB) children (B) and in children without and with liver steatosis (C) detected by ultrasound ($p < 0.0001$)

Table 2 Characteristics of the participants with and without liver steatosis detected on ultrasound

	No steatosis group (<i>N</i> =41)	Steatosis group (<i>N</i> =48)	<i>p</i> value
Demographic findings			
Group			<0.001
Normal	36 (87.80%)	4 (8.33%)	
Overweight/obesity	5 (12.20%)	44 (91.67%)	
Male	16 (39.02%)	39 (81.25%)	<0.001
Age (years)	15.17 [12.09; 16.61]	12.29 [11.04; 15.25]	0.025
Anthropometric measurements			
Weight (kg)	51.17 ± 9.44	68.33 ± 16.20	<0.001
Weight (z score)	−0.12 ± 1.54	1.82 ± 1.16	<0.001
Height (cm)	160.21 ± 10.51	159.04 ± 11.60	0.621
Height (z score)	0.31 ± 1.35	0.55 ± 1.14	0.354
BMI (kg/m ²)	20.01 ± 3.69	26.68 ± 3.60	<0.001
BMI (z score)	−0.40 [−1.73; 0.42]	1.99 [1.50; 2.47]	<0.001
WC (cm)	69.27 ± 8.61	89.23 ± 10.57	<0.001
WC to height	0.43 ± 0.06	0.56 ± 0.06	<0.001
Systolic BP (mmHg)	110.0 [106.0; 119.0]	110.0 [108.0; 119.0]	0.340
Diastolic BP (mmHg)	69.0 [61.0; 70.0]	61.5 [60.5; 70.0]	0.292
Blood biochemical profiles			
Glucose (mg/dL)	97.00 [91.00; 100.00]	97.00 [90.50; 103.00]	1.000
Uric acid (mg/dL)	5.33 ± 1.47	6.47 ± 1.86	0.002
AST (IU/L)	22.00 [19.00; 30.00]	41.00 [28.00; 62.50]	<0.001
ALT (IU/L)	13.00 [9.00; 24.00]	64.00 [35.50; 112.00]	<0.001
AST-to-ALT ratio	1.71 [1.12; 2.11]	0.64 [0.55; 0.79]	<0.001
γ-GT (IU/L)	12.00 [11.00; 19.00]	27.00 [22.00; 42.00]	<0.001
Total cholesterol (mg/dL)	155.46 ± 35.16	171.81 ± 30.49	0.023
Triglycerides (mg/dL)	79.00 [64.00; 113.00]	111.00 [91.00; 157.00]	<0.001
HDL cholesterol (mg/dL)	48.45 ± 10.29	45.53 ± 9.65	0.221
LDL cholesterol (mg/dL)	93.79 ± 26.06	108.60 ± 27.28	0.023
25-OH Vitamin D (ng/mL)	22.80 [18.80; 27.90]	15.00 [12.60; 21.55]	0.027
Radiologic findings by the US			
Liver steatosis grade			<0.001
No	41 (100.00%)	0 (0.0%)	
Mild	0 (0.0%)	9 (18.75%)	
Moderate	0 (0.0%)	34 (70.83%)	
Severe	0 (0.0%)	5 (10.42%)	
Attenuation imaging value			
Observer 1	0.50 ± 0.10	0.72 ± 0.12	<0.001
Observer 2	0.47 ± 0.09	0.72 ± 0.13	<0.001
NAFLD score			
Hepatic steatosis index	27.14 ± 5.17	39.59 ± 6.08	<0.001
Framingham steatosis index	3.23 [2.02; 4.68]	42.22 [29.16; 56.17]	<0.001

Data are expressed as the means ± standard deviations or medians (interquartile ranges) or *n* (%). *p* value was obtained from the Student *t* test, Wilcoxon rank-sum test, or chi-square test comparing the children with steatosis and without steatosis detected on ultrasound. *BMI*, body mass index; *WC*, waist circumference; *BP*, blood pressure; *AST*, aspartate aminotransferase; *ALT*, alanine aminotransferase; *γ-GT*, gamma-glutamyl transferase; *HDL*, high-density lipoprotein; *LDL*, low-density lipoprotein; *US*, ultrasound; *NAFLD*, nonalcoholic fatty liver disease

Fig. 4 Correlation of anthropometric measures, blood biochemical profiles, ultrasound findings, and hepatic steatosis indexes in normal weight and obese children. In this correlogram, positive correlations are expressed in blue, and negative correlations are expressed in red. The intensity of the colour is proportional to the correlation coefficients. The coefficients in the expressed variables are statistically significant (BMI, body mass index; WC, waist circumference; WC to Ht, waist circumference-to-height ratio; HSI, hepatic steatosis index; FSI, Framingham steatosis index; AST, aspartate aminotransferase; ALT, alanine aminotransferase; AST to ALT, AST-to-ALT ratio; GGT, γ -glutamyl transferase; HDL, high-density lipoprotein; LDL, low-density lipoprotein; TG, triglyceride; vitamin, 25-OH vitamin D; US, ultrasound; ATI, attenuation imaging values)



A

Variables	β (95% CI)	Constant	P value
Simple linear regression			
logAge	-0.23 (-0.41 - -0.05)	1.20	0.01
SEX	-0.20 (-0.20 - -0.07)	0.66	<0.001
BMI	0.021 (0.02-0.03)	0.11	<0.001
logALT	0.084 (0.06-0.11)	0.31	<0.001
HSI	0.01 (0.01-0.02)	0.18	<0.001
Uric Acid	0.03 (0.01-0.05)	0.41	<0.001
Multiple linear regression			
BMI	0.015 (0.009-0.021)	0.077	<0.001
logALT	0.049 (0.022-0.077)		<0.001

B

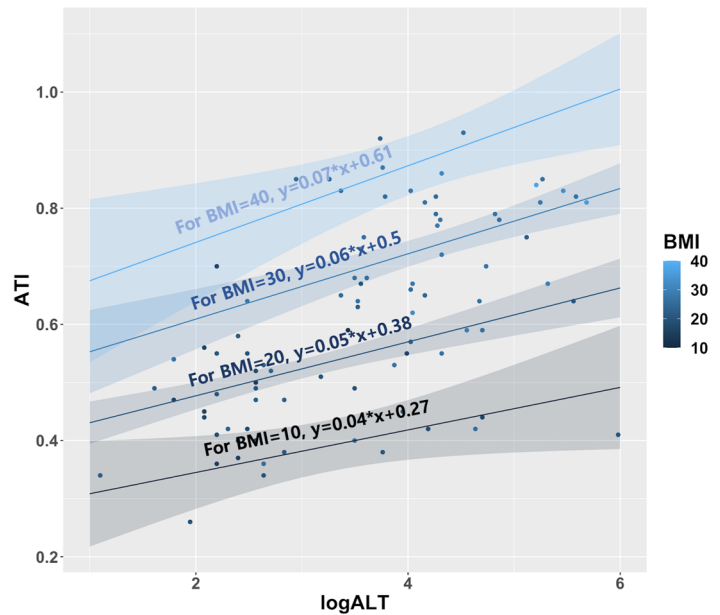


Fig. 5 A The association between attenuation imaging values (ATI) and age, sex, body mass index (BMI), alanine aminotransferase (ALT), hepatitis steatosis index (HSI), and uric acid using simple and

multiple linear regression. **B** The positive association between ATI and BMI and ALT using multiple linear regression

The association between ATI and the predictors using simple and multiple linear regression

When the predictors involved in the linear regression model were not normally distributed, the predictors were log-transformed. Simple linear regression analysis showed a significant association between ATI and age, sex, BMI, ALT, HSI, and uric acid ($p < 0.05$, Fig. 5A). Then, we performed stepwise multiple linear regression using backward elimination methods using the predictors (sex, log age, BMI, log ALT, HSI, and uric acid), which showed that the significant predictors were BMI and log ALT ($p < 0.05$). The multiple linear regression showed a significant positive association among BMI, log ALT, and ATI ($p < 0.05$, Fig. 5A). To visualise this model, we used the predict function in the R program, and Fig. 4B shows the significant positive associations between ATI and BMI and log ALT ($p < 0.05$, Fig. 5B).

The diagnostic performance of ATI for hepatic steatosis and the intraclass correlation between observers

The ROC analysis revealed that the area under the ROC curve (AUC) of the ATI was 0.923 (95% CI: 0.866–0.979), that of the HSI was 0.926 (95% CI: 0.864–0.988), that of the FSI was 0.921 (95% CI: 0.864–0.979), and that of BMI plus ALT was 0.866 (95% CI: 0.783–0.950) ($p < 0.05$, Fig. 6A). The best threshold (sensitivity, specificity) of ATI in the ROC analysis was 0.585 (90.2%, 85.4%), that for the HSI was 34.5 (95.1%, 87.5%), that for the FSI was 6.180 (85.4%, 89.6%), and that for BMI plus ALT was 44.285 (78.0%, 93.8%) (Fig. 6B). The comparison of the diagnostic performance using the ROC analysis showed no significant

differences between ATI and HSI, FSI, and BMI plus ALT according to pROC in the R program ($p > 0.05$). The intra-class correlation coefficient (ICC) of interobserver variability was 0.92 (95% CI: 0.88–0.95) between observers 1 and 2 ($p < 0.05$). The ICCs of intraobserver variability were 0.96 (95% CI: 0.94–0.97) for observer 1 and 0.93 (95% CI: 0.89–0.95) for observer 2 ($p < 0.05$).

Diagnostic performance of the noninvasive predictors for hepatic steatosis using Bayesian LCA

Due to the paucity of liver biopsy results, we analysed the diagnostic performance of noninvasive predictors for hepatic steatosis using two levels of Bayesian LCA with the imperfect gold-standard methodology. To fit the model, the predictors were changed to dichotomous variables. The ATI cut-off level was 0.59; US results were categorised as hepatic steatosis or not (grade 0, and grades 1, 2, 3). The HSI cut-off level was 35, and the FSI cut-off level was 23. BMI plus ALT was defined as overweight (BMI 85 percentile or more) plus ALT (male 30 or more, female 22.1 or more) [19, 20]. We constructed two models (model 1: ATI, US, FSI, and BMI plus ALT; model 2: ATI, US, HSI, and BMI plus ALT). In both models, ATI showed the best performance for predicting hepatic steatosis among other known noninvasive NAFLD predictors (Table 3).

Discussion

Our study suggests that ATI could be a novel method for the detection of hepatic steatosis in paediatric patients. In our study, ATI showed a significant association with BMI

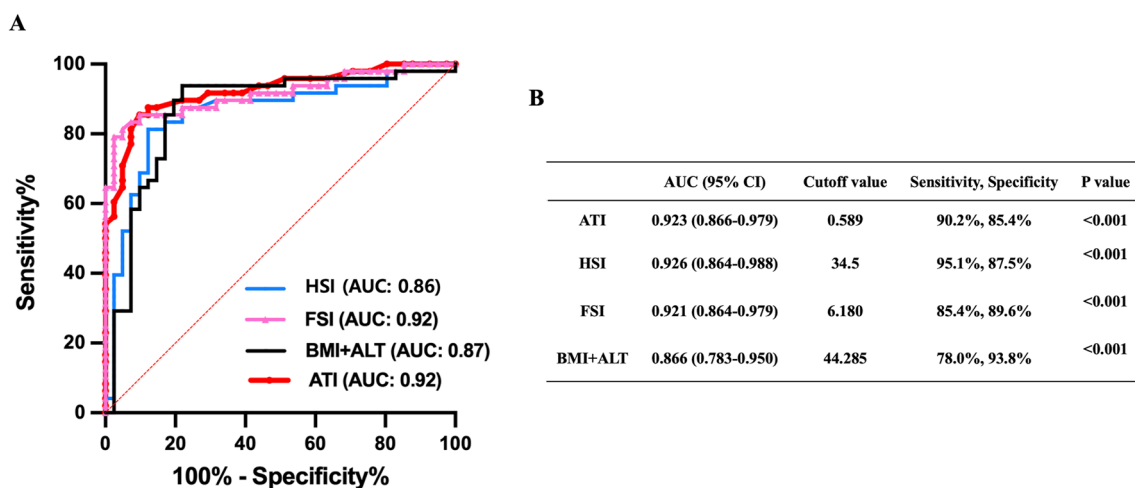


Fig. 6 Diagnostic performance of median ATI values for predicting hepatic steatosis by ultrasound (A, B). ATI, attenuation imaging; HSI, hepatic steatosis index; FSI, Framingham steatosis index; BMI, body

mass index; ALT, alanine aminotransferase; US, ultrasound; AUC, area under the curve; CI, confidence interval

Table 3 Diagnostic performance of the noninvasive predictors for liver steatosis according to the Bayesian latent class model analysis

Parameter	Sensitivity (95% CI)	Specificity (95% CI)	PPV (95% CI)	NPV (95% CI)	Performance*
Model 1					
ATI	89.1 (78.6–95.8)	100 (100–100)	100 (100–100)	87.7 (75.6–95.2)	89.1
US	89.6 (78.9–96.0)	92.5 (81.1–98.7)	94.0 (84.9–99.0)	87.1 (74.0–95.2)	82.1
FSI	77.4 (64.4–87.2)	97.3 (89.0–100)	97.4 (89.4–100)	76.7 (63.2–86.9)	74.7
BMI + ALT	81.0 (68.5–90.1)	99.3 (92.9–100)	99.4 (93.3–100)	80.0 (66.7–89.5)	80.3
Model 2					
ATI	89.4 (79.0–96.0)	100 (100–100)	100 (100–100)	88.0 (76.2–95.6)	89.4
US	89.7 (79.7–95.9)	92.3 (81.2–98.3)	93.8 (84.3–98.6)	87.5 (75.3–95.1)	82
HSI	85.6 (74.3–93.5)	99.4 (93.3–100)	99.5 (94.0–100)	84.2 (71.3–92.7)	85
BMI + ALT	81.5 (69.0–90.4)	99.4 (93.8–100)	99.4 (93.9–100)	80.6 (67.9–90.0)	80.9

PPV, positive predictive value; NPV, negative predictive value; 95% CI, 95% confidence interval; ATI, attenuation index; US, ultrasound; FSI, Framingham steatosis index; HSI, hepatic steatosis index; BMI, body mass index; ALT, alanine aminotransferase

*Performance = Sensitivity + Specificity – 100

and ALT in the multivariate regression analysis. When we compared diagnostic performance by Bayesian LCA with other screening methods, ATI was superior to US only, FSI, HSI, and BMI plus ALT.

Several studies have been conducted to find noninvasive screening methods for NAFLD, including the use of anthropometric and biochemical characteristics [21, 22]. Various characteristics in obese children, including elevated BMI, WC, serum ALT, alkaline phosphatase (ALP), insulin resistance, lipid profile, GGT, and uric acid levels, and decreased serum vitamin D levels, have been suggested as markers of NAFLD in children [21–26]. In our study, there were concordant significant differences in various anthropometric and biochemical markers between the normal weight and OW/OB groups and the group with and without steatosis according to US. The significant abnormalities in blood biochemical findings in the OW/OB group and subjects with hepatic steatosis according to US could imply that NAFLD may coexist or appear later. The significant differences in age and sex between the OW/OB and normal weight groups are associated with the fact that this study design did not use a matching method. In the statistical analysis, age and sex were considered covariates.

For the diagnosis of NAFLD, liver biopsy is the gold standard method for the quantification of hepatic steatosis [8, 27, 28]. Owing to limitations of liver biopsy, including sampling error and invasiveness, there have been several attempts to find an objective surrogate method to quantitatively evaluate hepatic steatosis. Currently, MR spectroscopy (MRS) and MRI proton density fat fraction (MRI-PDFF) have been regarded as possible tools [29–31]. However, MRI evaluation is expensive and time-consuming and, particularly in young children, often requires sedation [17, 24].

US is a widely used convenient method for evaluating hepatic steatosis. Greyscale US imaging allows for the

subjective estimation of the degree of hepatic steatosis. These methods are noninvasive but provide semiquantitative results, and occasionally, additional image data processing steps are needed. Recently, US-based methods for the quantification of hepatic steatosis have been developed by using the nature of the interaction of the US beam with tissue [32–36]. The controlled attenuation parameter (CAP) using FibroScan® and ATI are representative methods [24]. The quantity of fat droplets reflects changes in the viscoelastic characteristics of the liver [37]. CAP measures the attenuation of the US beam as it passes through the liver and reflects increased attenuation of the US beam in the liver with steatosis [24, 34]. However, in clinical situations, CAP has limitations of a lack of anatomical information and requires additional equipment to measure CAP [34].

ATI is a more up-to-date method than CAP, and it can provide objective information on hepatic steatosis with conventional greyscale echogenicity and structural information simultaneously [34]. According to several recent studies in adults, ATI demonstrated a good diagnostic performance and correlation with the degree of steatosis with reference values based on liver biopsy or MRI-PDFF [8, 24, 33–44]. Only one study has been conducted with children thus far; in the study by Song et al, ATI was found to be useful for the quantitative evaluation of hepatic steatosis in children as well [17]. The suggested cut-off value of AC to discriminate normal and fatty liver was 0.59 dB/cm/MHz and to discriminate moderate-to-severe and mild fatty liver was 0.69 dB/cm/MHz in their study [17]. In our study, the mean AC value in the normal group was 0.47–0.5, and that in the steatosis group was 0.72. This was the corresponding value in the normal group. Regarding the AC value in the steatosis group, we can consider that most of the patients in our study belonged to the moderate-to-severe fatty liver group, considering

that more than 80% of the patients had US grades 2 and 3 in our study, which also showed corresponding values. Our study results also showed significant correlations with BMI and ALT, with high ROC values. This is the first study to reveal the relationship between clinical features and ATI in children.

There were several advantages of using ATI as a quantitative tool in this clinical scenario. By measuring the degree of attenuation in different parts of the liver, a clinician can estimate the extent of liver steatosis and track changes over time, which can be helpful in monitoring the progression of the disease and guiding treatment decisions. Especially in paediatric clinical practice, the use of an attenuation tool reduces the need for sedation.

Our study has several limitations. First, we did not perform a histologic confirmation of hepatic steatosis in children, and therefore, we analysed the diagnostic performance of ATI using two levels of Bayesian LCA. Bayesian LCA can analyse the accuracy of each imperfect diagnostic test, as well as the dependence between tests, to simultaneously estimate disease prevalence and the sensitivity and specificity of all tests [45, 46]. Bayesian LCA uses known information about test performance and yields accuracy estimates that are easier to interpret. Second, we did not evaluate fibrosis [8]. In ATI, the AC value is determined only by hepatic steatosis, and the stage of fibrosis is not associated with AC. This is similar to the results of CAP [17, 29, 31]. In our study, there was no patient with cirrhosis on greyscale US. For obese children, it is important to detect and screen for NAFLD before NAFLD progresses to hepatic fibrosis. Therefore, it is more important to objectively evaluate hepatic steatosis initially. Third, a relatively small number of participants were included in our study. A larger study population is required to validate the ATI technique for paediatric NAFLD. Fourth, none of the patients had undergone MR study. Given the age of our study population, it was feasible for most patients to undergo MR study without sedation. However, this was not implemented due to time and cost constraints.

Conclusion

The results of our study show that the diagnostic performance of ATI in the detection of hepatic steatosis is higher than that of various imperfect gold standards in children. In addition, ATI has several merits for the evaluation of paediatric NAFLD compared to other methods, including its noninvasiveness, objective and precise ability to reflect the degree of hepatic steatosis, meaningful value with clinical indicators, and convenience.

Funding The research described in this publication was supported by the National Research Foundation of Korea (NRF) grant funded by the Ministry of Science and ICT (MSIT) (NRF-2021R1F1A1058240). The funding bodies had no role in the study design, collection, analysis, or interpretation of the data or writing of the manuscript.

Declarations

Guarantor The scientific guarantor of this publication is Ky Young Cho.

Conflict of interest The authors declare no financial or other competing interests.

Statistics and biometry One of the authors, Ky Young CHO, Ph.D., M.D., has significant statistical expertise.

Informed consent Written informed consent was obtained from all the participants and their parents on behalf of any participants under the age of 18 years old prior to the start of the study.

Ethics approval This study was carried out in accordance with the Declaration of Helsinki and approved by the Hallym University Kangnam Sacred Heart Hospital Institutional Review Board under IRB No. 2022–05–005.

Methodology

- prospective
- case-control study
- performed at one institution

References

1. Ferraioli G, Calcaterra V, Lissandrin R et al (2017) Noninvasive assessment of liver steatosis in children: the clinical value of controlled attenuation parameter. *BMC Gastroenterol* 17:61. <https://doi.org/10.1186/s12876-017-0617-6>
2. Yu EL, Schwimmer JB (2021) Epidemiology of pediatric nonalcoholic fatty liver disease. *Clin Liver Dis (Hoboken)* 17:196–199. <https://doi.org/10.1002/cld.1027>
3. Yu EL, Golshan S, Harlow KE et al (2019) Prevalence of non-alcoholic fatty liver disease in children with obesity. *J Pediatr* 207:64–70. <https://doi.org/10.1016/j.jpeds.2018.11.021>
4. Kiess W, Kirstein AS, Stein R, Vogel M (2022) Obesity after the Covid-19 pandemic and beyond. *J Pediatr Endocrinol Metab* 35:135–138. <https://doi.org/10.1515/jpem-2022-2135>
5. Gwag SH, Oh YR, Ha JW et al (2022) Weight changes of children in 1 year during COVID-19 pandemic. *J Pediatr Endocrinol Metab* 35:297–302. <https://doi.org/10.1515/jpem-2021-0554>
6. Feldstein AE, Charatcharoenwitthaya P, Treeprasertsuk S, Benson JT, Enders FB, Angulo P (2009) The natural history of non-alcoholic fatty liver disease in children: a follow-up study for up to 20 years. *Gut* 58:1538–1544. <https://doi.org/10.1136/gut.2008.171280>
7. Phen C, Ramirez CM (2021) Hepatic steatosis in the pediatric population: an overview of pathophysiology, genetics, and diagnostic workup. *Clin Liver Dis (Hoboken)* 17:191–195. <https://doi.org/10.1002/cld.1008>
8. Bae JS, Lee DH, Lee JY et al (2019) Assessment of hepatic steatosis by using attenuation imaging: a quantitative, easy-to-perform ultrasound technique. *Eur Radiol* 29:6499–6507. <https://doi.org/10.1007/s00330-019-06272-y>

9. Dasarathy S, Dasarathy J, Khiyami A, Joseph R, Lopez R, McCullough AJ (2009) Validity of real time ultrasound in the diagnosis of hepatic steatosis: a prospective study. *J Hepatol* 51:1061–1067. <https://doi.org/10.1016/j.jhep.2009.09.001>
10. Strauss S, Gavish E, Gottlieb P, Katsnelson L (2007) Interobserver and intraobserver variability in the sonographic assessment of fatty liver. *AJR Am J Roentgenol* 189:W320–323. <https://doi.org/10.2214/AJR.07.2123>
11. Rockey DC, Caldwell SH, Goodman ZD, Nelson RC, Smith AD (2009) Liver biopsy. *Hepatology* 49:1017–1044. <https://doi.org/10.1002/hep.22742>
12. Kim JH, Yun S, Hwang SS et al (2018) The 2017 Korean National Growth Charts for children and adolescents: development, improvement, and prospects. *Korean J Pediatr* 61:135–149. <https://doi.org/10.3345/kjp.2018.61.5.135>
13. Jeon D, Son M, Shim J (2021) Dynamics of serum retinol and alpha-tocopherol levels according to non-alcoholic fatty liver disease status. *Nutrients* 13:1720. <https://doi.org/10.3390/nu13051720>
14. Nima M, Mehdi N, Mohammad H et al (2021) The Ability of the Framingham Steatosis Index (FSI) to predict non-alcoholic fatty liver disease (NAFLD): a cohort study. *Clin Res Hepatol Gastroenterol* 45:101567. <https://doi.org/10.1016/j.clinre.2020.10.011>
15. Kim SH, Lee JM, Kim JH et al (2005) Appropriateness of a donor liver with respect to macrosteatosis: application of artificial neural networks to US images—initial experience. *Radiology* 234:793–803. <https://doi.org/10.1148/radiol.2343040142>
16. Hernaez R, Lazo M, Bonekamp S et al (2011) Diagnostic accuracy and reliability of ultrasonography for the detection of fatty liver: a meta-analysis. *Hepatology* 54:1082–1090. <https://doi.org/10.1002/hep.24452>
17. Song K, Son NH, Chang DR, Chae HW, Shin HJ (2022) Feasibility of ultrasound attenuation imaging for assessing pediatric hepatic steatosis. *Biology (Basel)* 11:1087. <https://doi.org/10.3390/biology11071087>
18. MORU (2011) MICE solution, Mahidol-Oxford Tropical Medicine Research Unit (MORU) and Mahidol University, Thailand. Available via <http://mice.tropmedres.ac/home.aspx>. Accessed 19 Oct 2022
19. Strauss RS, Barlow SE, Dietz WH (2000) Prevalence of abnormal serum aminotransferase values in overweight and obese adolescents. *J Pediatr* 136:727–73
20. Jung TY, Kim MS, Hong HP, Kang KA, Jun DW (2020) Comparative assessment and external validation of hepatic steatosis formulae in a community-based setting. *J Clin Med* 9:2851. <https://doi.org/10.3390/jcm9092851>
21. Weiss R, Dziura J, Burgert TS et al (2004) Obesity and the metabolic syndrome in children and adolescents. *N Engl J Med* 350:2362–2374. <https://doi.org/10.1056/NEJMoa031049>
22. Kim JY, Cho J, Yang HR (2018) Biochemical predictors of early onset non-alcoholic fatty liver disease in young children with obesity. *J Korean Med Sci* 33:e122. <https://doi.org/10.3346/jkms.2018.33.e122>
23. Vadarlis A, Chantavaridou S, Kalopitas G et al (2022) The anthropometric and biochemical profile of pediatric non-alcoholic fatty liver disease: a systematic review and a meta-analysis. *Clin Nutr* 41:105–121. <https://doi.org/10.1016/j.clnu.2021.11.016>
24. Sasso M, Beaugrand M, de Ledinghen V et al (2010) Controlled attenuation parameter (CAP): a novel VCTE™ guided ultrasonic attenuation measurement for the evaluation of hepatic steatosis: preliminary study and validation in a cohort of patients with chronic liver disease from various causes. *Ultrasound Med Biol* 36:1825–1835. <https://doi.org/10.1016/j.ultrasmedbio.2010.07.005>
25. Fiamenghi VI, Mello ED (2021) Vitamin D deficiency in children and adolescents with obesity: a meta-analysis. *J Pediatr (Rio J)* 97:273–279. <https://doi.org/10.1016/j.jped.2020.08.006>
26. Wortsman J, Matsuoka LY, Chen TC, Lu Z, Holick MF (2000) Decreased bioavailability of vitamin D in obesity. *Am J Clin Nutr* 72:690–693. <https://doi.org/10.1093/ajcn/72.3.690>
27. Kleiner DE, Brunt EM, Van Natta M et al (2005) Design and validation of a histological scoring system for nonalcoholic fatty liver disease. *Hepatology* 41:1313–1321. <https://doi.org/10.1002/hep.20701>
28. Kramer H, Pickhardt PJ, Kliewer MA et al (2017) Accuracy of liver fat quantification with advanced CT, MRI, and ultrasound techniques: prospective comparison with MR spectroscopy. *AJR Am J Roentgenol* 208:92–100. <https://doi.org/10.2214/AJR.16.16565>
29. Caussy C, Alquirraish MH, Nguyen P et al (2018) Optimal threshold of controlled attenuation parameter with MRI-PDFF as the gold standard for the detection of hepatic steatosis. *Hepatology* 67:1348–1359. <https://doi.org/10.1002/hep.29639>
30. Ferraioli G, Maiocchi L, Raciti MV et al (2019) detection of liver steatosis with a novel ultrasound-based technique: a pilot study using MRI-derived proton density fat fraction as the gold standard. *Clin Transl Gastroenterol* 10:e00081. <https://doi.org/10.14309/ctg.0000000000000081>
31. Park J, Lee JM, Lee G, Jeon SK, Joo I (2022) Quantitative evaluation of hepatic steatosis using advanced imaging techniques: focusing on new quantitative ultrasound techniques. *Korean J Radiol* 23:13–29. <https://doi.org/10.3348/kjr.2021.0112>
32. Fujiwara Y, Kuroda H, Abe T et al (2018) The B-mode image-guided ultrasound attenuation parameter accurately detects hepatic steatosis in chronic liver disease. *Ultrasound Med Biol* 44:2223–2232. <https://doi.org/10.1016/j.ultrasmedbio.2018.06.017>
33. Tamaki N, Koizumi Y, Hirooka M et al (2018) Novel quantitative assessment system of liver steatosis using a newly developed attenuation measurement method. *Hepatol Res* 48:821–828. <https://doi.org/10.1111/hepr.13179>
34. Jeon SK, Lee JM, Joo I (2021) Clinical feasibility of quantitative ultrasound imaging for suspected hepatic steatosis: intra- and inter-examiner reliability and correlation with controlled attenuation parameter. *Ultrasound Med Biol* 47:438–445. <https://doi.org/10.1016/j.ultrasmedbio.2020.11.009>
35. Ghoshal G, Lavarello RJ, Kemmerer JP, Miller RJ, Oelze ML (2012) Ex vivo study of quantitative ultrasound parameters in fatty rabbit livers. *Ultrasound Med Biol* 38:2238–2248
36. Ferraioli G, Maiocchi L, Saviotto G et al (2021) Performance of the attenuation imaging technology in the detection of liver steatosis. *J Ultrasound Med* 40:1325–1332. <https://doi.org/10.1016/j.ultrasmedbio.2012.08.010>
37. Lédinghen V, Vergniol J, Foucher J, Merrouche W, Bail B (2012) Non-invasive diagnosis of liver steatosis using controlled attenuation parameter (CAP) and transient elastography. *Liver Int* 32:911–918. <https://doi.org/10.1111/j.1478-3231.2012.02820.x>
38. Jeon SK, Lee JM, Joo I et al (2019) Prospective evaluation of hepatic steatosis using ultrasound attenuation imaging in patients with chronic liver disease with magnetic resonance imaging proton density fat fraction as the reference standard. *Ultrasound Med Biol* 45:1407–1416. <https://doi.org/10.1016/j.ultrasmedbio.2019.02.008>
39. DioguardiBurgio M, Ronot M, Reizine E et al (2020) Quantification of hepatic steatosis with ultrasound: promising role of attenuation imaging coefficient in a biopsy-proven cohort. *Eur Radiol* 30:2293–2301. <https://doi.org/10.1007/s00330-019-06480-6>
40. Jesper D, Klett D, Schellhaas B et al (2020) Ultrasound-based attenuation imaging for the non-invasive quantification of liver fat

- a pilot study on feasibility and inter-observer variability. *IEEE J Transl Eng Health Med* 8:1800409. <https://doi.org/10.1109/JTEHM.2020.3001488>
41. Tada T, Kumada T, Toyoda H et al (2020) Attenuation imaging based on ultrasound technology for assessment of hepatic steatosis: a comparison with magnetic resonance imaging-determined proton density fat fraction. *Hepatol Res* 50:1319–1327. <https://doi.org/10.1111/hepr.13563>
 42. Tada T, Kumada T, Toyoda H et al (2019) Utility of attenuation coefficient measurement using an ultrasound-guided attenuation parameter for evaluation of hepatic steatosis: comparison with MRI-determined proton density fat fraction. *AJR Am J Roentgenol* 212:332–341. <https://doi.org/10.2214/AJR.18.20123>
 43. Jeon SK, Lee JM, Joo I, Park SJ (2021) Quantitative ultrasound radiofrequency data analysis for the assessment of hepatic steatosis in nonalcoholic fatty liver disease using magnetic resonance imaging proton density fat fraction as the reference standard. *Korean J Radiol* 22:1077–1086. <https://doi.org/10.3348/kjr.2020.1262>
 44. Tada T, Iijima H, Kobayashi N et al (2019) Usefulness of attenuation imaging with an ultrasound scanner for the evaluation of hepatic steatosis. *Ultrasound Med Biol* 45:2679–2687. <https://doi.org/10.1016/j.ultrasmedbio.2019.05.033>
 45. Dendukuri N, Schiller I, de Groot J et al (2018) Concerns about composite reference standards in diagnostic research. *BMJ* 360:j5779. <https://doi.org/10.1136/bmj.j5779>
 46. Yang I, Becker MP (1997) Latent variable modeling of diagnostic accuracy. *Biometrics* 53:948–958
- Publisher's note** Springer Nature remains neutral with regard to jurisdictional claims in published maps and institutional affiliations.
- Springer Nature or its licensor (e.g. a society or other partner) holds exclusive rights to this article under a publishing agreement with the author(s) or other rightsholder(s); author self-archiving of the accepted manuscript version of this article is solely governed by the terms of such publishing agreement and applicable law.